Dalton Transactions

RSC Publishing

PAPER

View Article Online
View Journal | View Issue

Cite this: *Dalton Trans.*, 2013, **42**, 4163

Understanding intermolecular C–F bond activation by a transient titanium neopentylidyne: experimental and theoretical studies on the competition between 1,2-CF bond addition and [2 + 2]-cycloaddition/β-fluoride elimination†

Hongjun Fan,*[a] Alison R. Fout,[b] Brad C. Bailey,[b] Maren Pink,[b] Mu-Hyun Baik*[b] and Daniel J. Mindiola*[b]

Complex (PNP)Ti=CH^{t}Bu(CH$_2$^{t}Bu) (PNP$^-$ = N[2-P(CHMe$_2$)$_2$-4-methylphenyl]$_2$) eliminates H$_3$C^{t}Bu to form transient (PNP)Ti≡C^{t}Bu, which activates the C–F bond of *ortho*-difluoropyridine and *ortho*-fluoropyridine to form the alkylidene–fluoride complexes, (PNP)Ti=C[^{t}Bu(NC$_5$H$_3$F)](F) (**1**) and (PNP)Ti=C[^{t}Bu(NC$_5$H$_4$)](F) (**2**), respectively. When (PNP)Ti=CH^{t}Bu(CH$_2$^{t}Bu) is treated with *meta*-fluoropyridine, the ring-opened product (PNP)Ti(C(^{t}Bu)CC$_4$H$_3$-3-FNH) (**3**) is the only recognizable titanium metal complex formed. Theoretical studies reveal that pyridine binding disfavors 1,2-CF bond addition across the alkylidyne ligand in the case of *ortho*-fluoride pyridines, while sequential [2 + 2]-cycloaddition/β-fluoride elimination is a lower energy pathway. In the case of *meta*-fluoropyridine, [2 + 2]-cycloaddition and subsequent ring-opening metathesis is favored as opposed to C–H bond addition or sequential [2 + 2]-cycloaddition/β-hydride elimination. In all cases, C–H bond addition of *ortho*-fluoropyridines or *meta*-fluoropyridine is discouraged because such substrate must bind to titanium *via* its C–H bond, which is rather weak compared to the titanium–pyridine binding.

Received 26th October 2012,
Accepted 14th January 2013

DOI: 10.1039/c3dt32570a

www.rsc.org/dalton

1. Introduction

Activating carbon–fluorine bonds in aromatic substrates represents a significant challenge in organotransition metal chemistry in part because it is one of the strongest bonds with typical bond energies of ~125 kcal mol^{-1}. Carbon–fluorine bonds are typically inert and highly resistant to common degradation pathways including oxidation.[1] The chemical inertness of fluorocarbons is exacerbated by their poor binding affinities to Lewis acids[1] and identifying a system that can activate C–F bonds, especially selectively, constitutes an attractive area of research not only from applied but also from fundamental standpoint. Not surprisingly, complexes bearing metal–carbon multiple bonds that are capable of C–F bond activation are exceedingly rare with the only reported example being the transient titanium alkylidyne (PNP)Ti≡C^{t}Bu (**A**) (PNP$^-$ = N[2-P(CHMe$_2$)$_2$-4-methylphenyl]$_2$) that we disclosed previously.[2,3] We showed that **A** can cleave the C–F linkage in perfluoro substrates like C$_6$F$_6$ and CF$_3$C$_6$F$_5$, under mild conditions to afford rare examples of disubstituted alkylidene–fluorides, (PNP)Ti=C[^{t}Bu(Ar$_F$)](F) (Ar$_F$ = C$_6$F$_5$, *p*-CF$_3$C$_6$F$_4$) depicted in Scheme 1.[2,3] In these cases, mixtures of *syn* and *anti* alkylidene rotamers were observed in solution that slowly interconvert and a study of the mechanism of rotation was reported recently.[3] Gratifyingly, fractional crystallization allowed for isolation and crystallographic characterization of the *syn* rotamer in the case of (PNP)Ti=C[^{t}Bu(C$_6$F$_5$)](F), while both the *syn* and *anti* rotamer could be isolated for (PNP)Ti=C-[^{t}Bu(*p*-CF$_3$C$_6$H$_4$)](F) thus allowing us to study each isomer as well as the mechanism for alkylidene rotation.[2,3]

The only other example of 1,2-CF bond addition across a metal–ligand multiple bond was reported by Bergman and coworkers using the racemic *ansa*-metallocene imido (ethylenebis(tetrahydro)indenyl)Zr=N^{t}Bu (which is generated in solution) and NC$_5$F$_5$, to form the amide fluoride (ethylenebis(tetrahydro)indenyl)Zr(N^{t}Bu[NC$_5$F$_4$])F (Scheme 2).[4] C–F bond breaking was proposed to be driven by a combination of the inherent reactivity of the pyridine C–F motif as well as

[a]*State Key Laboratory of Molecular Reaction Dynamics, Dalian Institute of Chemical Physics, Chinese Academy of Sciences, Dalian, China. E-mail: fanhj@dicp.ac.cn*
[b]*Department of Chemistry, the Molecular Structure Center, and the School of Informatics, Indiana University, Bloomington, IN 47405, USA. E-mail: mbaik@indiana.edu, mindiola@indiana.edu*

†Electronic supplementary information (ESI) available: Pertinent DFT studies are available. See DOI: 10.1039/c3dt32570a

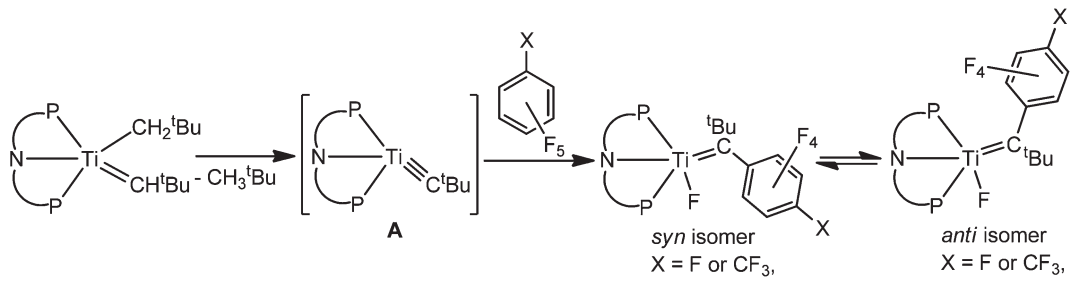

Scheme 1 1,2-CF addition across a transient titanium alkylidyne to afford a mixture of alkylidene isomers (rotamers).

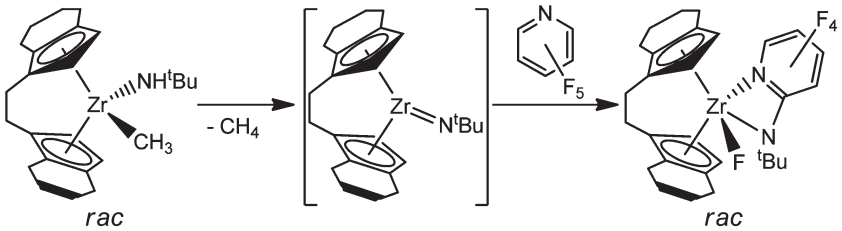

Scheme 2 1,2-CF addition across a transient zirconium imido.

formation of a very strong Zr–F bond.[4] Given the similarity of our reaction to that of the Bergman system, we may speculate that both processes follow similar pathways. However, the coordinating abilities of perfluoropyridine *versus* perfluoroarene should render these two reactions intuitively different especially if a binding event precedes C–F bond activation. In this work we demonstrate by applying a combination of experimental and theoretical studies that the mechanism of C–F bond activation can be highly dependent on a binding event of the substrate. We have found that coordination of an *ortho* substituted fluoropyridine to the Ti center in **A** can result in another competitive pathway: [2 + 2]-cycloaddition of the aromatic N–C bond across Ti≡C followed by a β-fluoride elimination step. This pathway contrasts the more commonly proposed 1,2-CX (X = H, F, *etc.*) bond addition pathway across early-transition metal imides,[4,5] alkylidenes,[6] and more recently, alkylidynes.[2,7,8] Based on this observation we convincingly demonstrate that [2 + 2]-cycloaddition is a viable pathway along the C–F bond activation of the *ortho* fluoropyridine while 3-fluoropyridine undergoes ring-opening metathesis of the *N*-heterocycle to form a three-seven-metallaazabicyclic.

2. Results and discussion

As documented in a prior publication,[2,3] the alkylidene complex (PNP)Ti=C[^{t}Bu(C_6F_5)](F), generated from C–F bond activation of C_6F_6 across the alkylidyne ligand in **A**, is most likely formed *via* 1,2-CF bond addition across the alkylidyne ligand. Computationally, it was found that a concerted [2 + 2]-cycloaddition step was uphill by 26.2 kcal mol^{-1} and notably higher in energy than the 22.4 kcal mol^{-1} value obtained for the 1,2-CF bond addition pathway. The latter barrier is also considerably lower than that for α-abstraction (27.8 kcal mol^{-1}), which is known to be the overall rate-determining step.

To assess whether or not binding of the substrate could alter the pathway along the C–F activation reaction we explored the reactivity of transient **A** with *ortho*-fluoro substituted pyridines. Pyridines carrying fluoro groups in the *ortho* position is logical to use as reagents since we have demonstrated previously that pyridine and picolines (*meta* and *para*) can be cleanly ring-opened *via* a [2 + 2] cycloaddition pathway of *N*-heterocycle by a transient titanium neopentylidyne **A**.[9] As noted earlier, Bergman and co-workers reported the C–F activation of NC_5F_5 by racemic (ethylenebis(tetrahydro)indenyl) Zr=N^{t}Bu, but the mechanism leading to bond cleavage of the substrate was never addressed.[4] If binding followed by cycloaddition of the *N*-heterocycle were the steps preceding the C–F bond activation reaction, then a β-fluoride elimination process should be culminating this type of reaction.

Experimentally it was found that treatment of (PNP)-Ti=CH^{t}Bu($CH_2{}^t$Bu) with neat *ortho* difluoropyridine resulted in gradual formation of a new product as implied by the ^{31}P NMR spectrum (33.6 and 29.4 ppm, $^2J_{PP}$ = 50 Hz). After 24 hours, workup of the reaction mixture afforded the disubstituted alkylidene–fluoride (PNP)Ti=C[^{t}Bu(NC_5H_3F)](F) (**1**) in 56% yield as a purple colored powder (Scheme 3). Evidence for formation of an alkylidene is clearly visible in the ^{13}C NMR spectrum (312.3 ppm with no $^1J_{C-H}$), while formation of a fluoride ligand is manifested by a significantly downfield shifted ^{19}F NMR spectroscopic resonance at 202.3 ppm. To determine the exact coordination geometry about the titanium center, we resorted to single crystal X-ray structural analysis. C–F activation at the *ortho* position is clearly evident from the solid-state diagram (Fig. 1). Unfortunately, several crystals were examined, and all were badly split to varying degrees and the crystal used finally for data collection consisted of one major

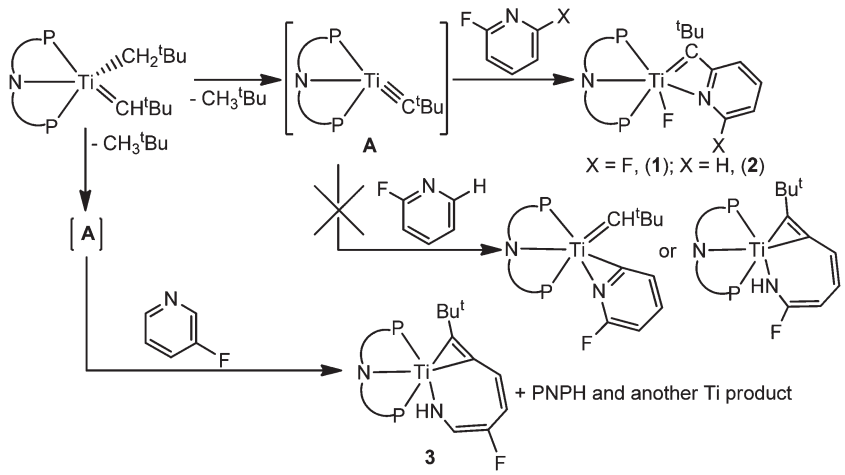

Scheme 3 Synthesis of complex **1** and **2** by C–F activation, as well as the fluorosubstituted ring-opened product, **3**.

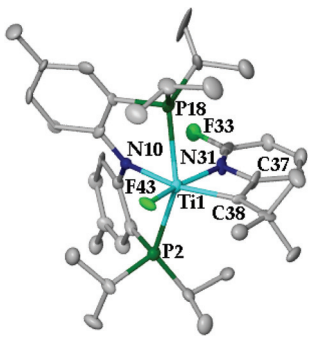

Fig. 1 Solid state structures of compounds **1** depicting thermal ellipsoids at the 35% probability level. H-atoms and a hexane solvent molecule have been omitted for clarity. Given the poor quality of the data set, metrical parameters are not listed.

component with numerous peaks due to minor fragments. Consequently, metrical parameters are not discussed or shown but the solid state structural diagram of complex **1** reveals C–F bond activation and formation of a six-coordinate titanium center whereby the fluoride, alkylidene and pyridine motif are virtually in a *mer*-configuration.‡ Formation of a azatitanacyclobutadiene scaffold in **1** most likely prevents the spectroscopic observation of alkylidene isomers (rotamers).[10]

If one *ortho* fluoro group in pyridine is replaced with H, the same type of transformation occurs. Accordingly, treating (PNP)Ti=CH^{t}Bu(CH$_2$^{t}Bu) with *ortho* fluoropyridine also results in exclusive C–F activation to form (PNP)Ti=C[^{t}Bu(NC$_5$H$_4$)](F) (**2**) in 43% yield (Scheme 3). No evidence for ring-opening of the *N*-heterocycle to form (PNP)Ti(C(^{t}Bu)CC$_4$H$_3$-2-FNH) or the hypothetical fluoro substituted pyridyl (PNP)Ti=CH^{t}Bu-(η^2-NC$_6$H$_3$F) were observed when the reaction is monitored by ^{31}P NMR spectroscopy (Scheme 3 shows these possible products). This result argues for C–F bond activation of the *N*-heterocycle being preferred over C–H activation or ring-opening metathesis (Scheme 3). Multinuclear NMR spectroscopic features for **2** are analogous to that observed for **1**: the alkylidene carbon resonance resolved at 313.6 ppm in the ^{13}C NMR spectrum, while the fluoride ligand was found at 178.6 ppm in the ^{19}F NMR spectrum. Although we were unsuccessful in obtaining solid state structural data for **2**, the observation of these salient spectroscopic features in addition to the similarities in the ^{31}P NMR spectrum (32.5 and 28.9 ppm, J_{PP} = 66 Hz) suggest this compounds to have an analogous geometry to complex **1**.

Since intermediate **A** can activate the C–F bond in *ortho* substituted fluoropyridines, we explored similar substrates having the fluoro group farther away from the nitrogen of the heterocycle. Using such substrates would also probe for whether an intermediate such as **A** could potentially ring-open the *N*-heterocycles, given that pyridine and picolines are known to undergo [2 + 2]-cycloaddition of the N=C bond across the Ti≡C^{t}Bu ligand.[9] When *m*-fluoropyridine is added to the alkylidyne precursor, (PNP)Ti=CH^{t}Bu(CH$_2$^{t}Bu), the three-seven-metallaazabicyclic compound (PNP)Ti(C(^{t}Bu)-CC$_4$H$_3$-3-FNH) (**3**) is spectroscopically observed (27%) in a mixture of PNPH (65%), and another metal based product (8%) which we have been unable to identify and which is not the C–F bond activated alkylidene compound (PNP)Ti=C[^{t}Bu-(NC$_5$H$_4$)](F). Although the reaction appears to produce mostly demetallated material, our NMR spectroscopic data are convincing enough to suggest one of the products to be the ring-opened complex **3**. In addition to inequivalent ^{31}P NMR spectroscopic environments (35.2 and 24.5 ppm, J_{P-P} = 42 Hz), the ^{1}H NMR spectrum confirms three sp^2-CH groups to be present in the seven-azamembered ring as well as the NH resonance (9.9 ppm). ^{19}F NMR spectroscopy argues against metal–fluoride bond formation, since no downfield resonance is observed (two products with chemical shifts −137.5 and −113.5 ppm are

‡Data for **1**·hexane: Monoclinic, *P*21/*c*, *T* = 128(2) K, *a* = 17.847(6) Å, *b* = 13.650 (4) Å, *c* = 18.883(7) Å, $\alpha = \gamma = 90°$, β = 108.742(13)°, *Z* = 4, *V* = 4356(2) Å^3, absorption coefficient = 0.303 mm^{-1}, *F*(000) = 1496, R_{int} = 0.4082; a total of 15 387 reflections collected in the range 2.21° < θ < 27.57°, of which 8962 were unique. GOF = 0.649, R_1 = 0.1057 [for observed 1366 reflections with $I > 2\sigma(I)$] and wR_2 = 0.1848 (for all data), largest diff. peak and hole = 0.0.039/−0.034.

spectroscopically observed). Therefore, this result indicates that replacement of F for H in the *ortho* position of the *N*-heterocycle can affect the site of activation (*i.e.* C=N *vs.* C–F), albeit the reaction is not clean.

To probe for the preference of C–F activation *vs.* ring-opening metathesis as well as the selectivity for C–F activation in fluorocarbons *vs.* fluorosubstituted pyridines, a series of a competition experiments were conducted. When complex (PNP)Ti=CH^{t}Bu(CH$_2$^{t}Bu) was treated with an equal molar mixture of pyridine and *o*-fluoropyridine, ring-opening metathesis to form the known species (PNP)Ti(C(^{t}Bu)CC$_4$H$_4$NH) was virtually quantitative (95% assayed by ^{31}P NMR spectroscopy),[9] with only 5% of the solution representing the C–F activation product **2**. However, partiality for C–F activation is observed when (PNP)Ti=CH^{t}Bu(CH$_2$^{t}Bu) is dissolved in an equal molar mixture of *o*-fluoropyridine and C_6F_6 to yield 80% of **2** *vs.* only 20% of (PNP)Ti=C[^{t}Bu(C_6F_5)](F). Thus, ring-opining C=N bond activation is preferred over C–F bond cleavage, and the binding of the pyridine moiety plays an important role in the selectivity of C–F bond activation (both intra and intermolecularly).

Experimentally identifying microscopic details about the pathway of C–F activation is challenging in part given the difficulties of isotopically labeling both the C or F sites. Furthermore, we established previously that formation of **A** is rate-determining based on KIE values obtained using (PNP)Ti=CH^{t}Bu(CH$_2$^{t}Bu)/(PNP)Ti=CD^{t}Bu(CD$_2$^{t}Bu) in the C–H activation reaction of benzene (KIE = 3.7, room temperature) and the pyridine ring-opening metathesis (KIE = 3.85, room temperature), which renders subsequent steps difficult to investigate, as these would be all post rate-determining. We therefore turned to high-level DFT studies to assess how the substrate of choice, *o*-fluoropyridine, influenced the pathway for each reaction. Since the α-hydrogen abstraction step to obtain the key intermediate **A** has been addressed in detail in previous work,[7] our discussion will focus on reactions after forming **A**. We are well aware that solvent medium could greatly affect the energies of all intermediates. We utilize a continuum solvation model to account for some of these effects using the dielectric constants of C_6F_6 and C_6H_6 to approximate *o*-fluoropyridine solvent. We have quantified these effects for example for the α-hydrogen abstraction step to obtain the key intermediate **A** in our previous work.[7] In benzene the computed barrier is 27.8 kcal mol^{-1}, which is in reasonable agreement with the experimental value of 24.6 kcal mol^{-1}. Intermediate **A** is 4.6 kcal mol^{-1} higher in free energy than (PNP)Ti=CH^{t}Bu(CH$_2$^{t}Bu). In *o*-fluoropyridine the computed barrier is 27.7 kcal mol^{-1}, and **A** is only 1.5 kcal mol^{-1} higher in energy compared to (PNP)Ti=CH^{t}Bu(CH$_2$^{t}Bu) (Fig. 2).

In contrast to mechanistic investigations of the C–F activation of C_6F_6, in which the [2 + 2]-cycloaddition step is less preferred,[3] our studies using *o*-fluoropyridine as the substrate suggest the opposite trend. Shown in Fig. 2 are three computed profiles for the reactivity of (PNP)Ti=CH^{t}Bu(CH$_2$^{t}Bu) with *o*-fluoropyridine: binding of *o*-fluoropyridine to **A** (solid line), 1,2-CF bond addition of *o*-fluoropyridine across the alkylidyne ligand of **A** (dashed line), and the [2 + 2]-cycloaddition/β-fluoride elimination pathway (bold solid line). From the reaction coordinate in Fig. 2 it is apparent that the [2 + 2]-cycloaddition/β-fluoride elimination pathway is energetically more feasible for forming complex **2**. Binding of *o*-fluoropyridine (**py$_F$**) nitrogen to transient **A** results in formation of nearly isoenergetic intermediate **A-py$_F$**. Although **A-py$_F$** is a reasonable intermediate to propose, we found that it is not relevant to either pathway involving C–F bond activation since the site of activation points away from the titanium alkylidyne moiety (solid line, Fig. 2). The preferred orientation of the substrate for the [2 + 2]-cycloaddition and β-fluoride elimination

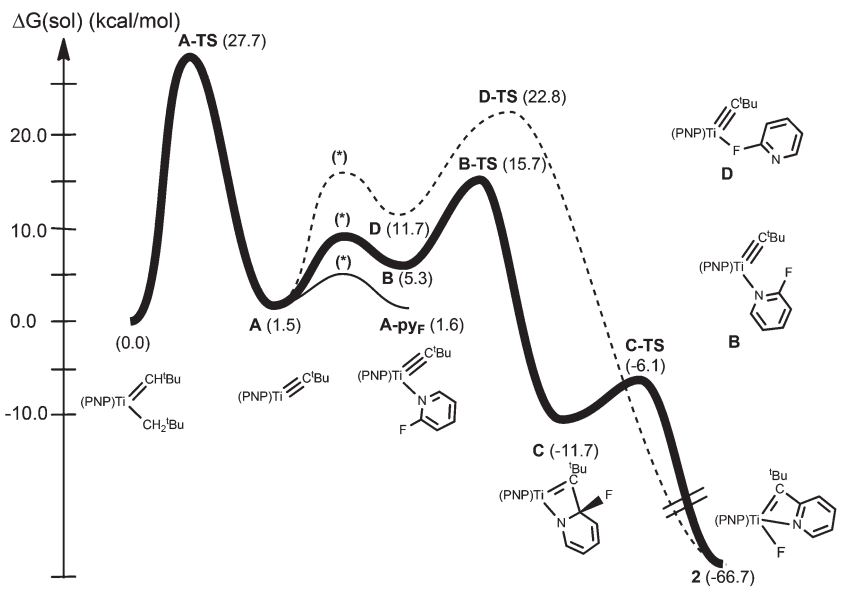

Fig. 2 C–F activation pathways of *o*-fluoropyridine by transient **A**. Solvent dielectric constant was set to 23.2 to emulate *o*-fluorobenzene.

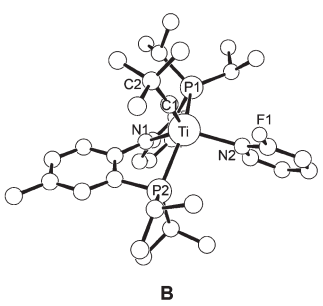

B

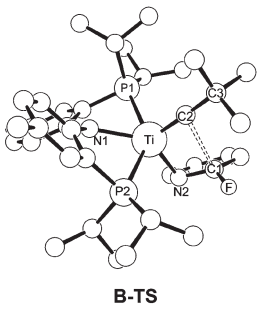

B-TS

Fig. 3 Computed structures for the key intermediate and transition state species along the [2 + 2]-cycloaddition/β-F elimination pathway involving *o*-fluoropyridine activation (distances in Å). For **B**: Ti–C1 1.75, Ti–P1 2.66, Ti–P2 2.60, Ti–N2 2.30. **B-TS**: Ti–N2 2.17, Ti–C2 1.77, Ti–P1 2.70, Ti–P2 2.65, C1–N2 1.35, C1–C2 2.87, C1–F 1.36.

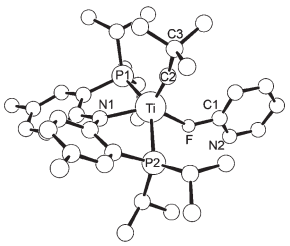

D

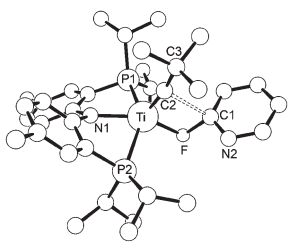

D-TS

Fig. 4 Computed structures for the intermediate and transition state species along the 1,2-CF bond addition pathway involving *o*-fluoropyridine activation (distances in Å). For **D**: Ti–F, 2.26; Ti–C2, 1.75; Ti–P1, 2.62; Ti–P2, 2.59; Ti–N1, 2.09. For **D-TS**: Ti–F, 2.04; Ti–C2 1.77; Ti–P1, 2.66; Ti–P2, 2.61; Ti–N1, 2.09; F–C1, 1.55; C1–C2, 2.48.

pathway involves intermediate **B**, which is the pyridine rotamer of **A-py$_F$** having the fluoride group pointing towards the alkylidyne ligand, and lying 3.7 kcal mol^{-1} higher in energy. Upon isomerization the subsequent [2 + 2]-cycloaddition step is overall exergonic (−11.7 kcal mol^{-1}, **C**), with a barrier of 10.4 kcal mol^{-1}, while the β-fluoride elimination step is virtually barrier less (5.6 kcal mol^{-1}) to furnish the very stable alkylidene product **2** (−66.7 kcal mol^{-1}). In the 1,2-CF addition pathway, a pre-binding event involving a linkage isomer of *o*-fluoropyridine **1-py$_F$** is required to afford **D**, which is energetically disfavored by 10.1 kcal mol^{-1} compared to the lowest energy N-bound adduct **A-py$_F$**. Stemming from **D**, the 1,2-CF bond addition across the Ti≡C^{t}Bu ligand must traverse an additional 11.1 kcal mol^{-1} in order to form **2**.

Taken altogether, the C–F activation pathway for the sequential steps [2 + 2] cycloaddition/β-F elimination is associated with a barrier of only 15.7 kcal mol^{-1}, which is considerably lower than the predicted 20.5 kcal mol^{-1} for the 1,2-CF bond addition pathway. The barriers predicted in Fig. 2 suggest that the binding of pyridine *via* its lone pair disfavors the 1,2-CF addition pathway, in part because of an extra dissociative step required to form an F-bound *o*-fluoropyridine adduct such as **D**. If the actual discrepancy in energies in the proposed adducts **B** and **D** were smaller than our computed estimate of ∼6 kcal mol^{-1}, the $\Delta\Delta G^{\ddagger}$ between the activated complexes **B-TS** and **D-TS** (7.1 kcal mol^{-1}) would be also smaller, therefore rendering the 1,2-CF bond addition pathway more competitive with respect to the [2 + 2]-cycloaddition pathway. Our computed reaction coordinate also predicts the overall rate-determining step for each pathway to be α-hydrogen abstraction to obtain transient **A**, which was expected based on the similar $t_{1/2}$ values obtained at 25 °C *versus* the C–H activation of benzene ($t_{1/2}$ = 3.0–3.2 h).[7] Fig. 3 depicts the proposed structures of the adduct **B** resulting from *o*-fluoropyridine binding to **A**, as well as the transition state structure leading to [2 + 2]-cycloaddition (**B-TS**). Overall, these structures are quite similar to the corresponding structures for the ring opening reaction of pyridine,[9] except here a C–H bond was replace by a C–F bond.

Fig. 4 depicts the proposed structures of the adduct resulting from *o*-fluoropyridine binding to **A** (compound **D**), as well as the transition state structure leading to 1,2-CF bond addition across the alkylidyne ligand (**D-TS**). We have compared metrical parameters of these two species with those obtained computationally using C_6F_6 [3] since the latter substrate shows preference for the 1,2-CF bond addition pathway. Shown in Table 1 are the computed binding free energy of *o*-fluoropyridine (+10.2 kcal mol^{-1}), which is better than that computed for C_6F_6 that is used as a reference (+14.1 kcal mol^{-1}).[3] The stronger binding for *o*-fluoropyridine is also reflected by the shorter Ti–F bond length of 2.26 Å (Fig. 3), and which is shorter to the distance 2.43 Å for alkylidyne adduct of C_6F_6.[3,11] This disparity in the bond lengths can be attributed to the more nucleophilic fluorine center, which is judged by the electrostatic potential (ESP) charge it bears (computed ESP charges on one F atom: *o*-fluoropyridine: −0.234; C_6F_6: −0.085). Interestingly, substrate binding weakens the sp^2 C–F bond, as shown by the computed C–F Mayer bond order in free *o*-fluoropyridine (0.96) versus 0.72 in **D**. Although *o*-fluoropyridine binds stronger to **A** *via* its fluorine site, its degree of activation can be best judged by the computed ΔG^{sol}-(activation) values shown in Table 1. For instance, the

Table 1 Computed free energies (in kcal mol^{-1}) for substrate binding and C–F bond activation

Pathway	Substrate	ΔG^{sol}(binding)	ΔG^{sol}(activation)	Activation barrier with respect to (PNP)Ti=CH^{t}Bu(CH$_2$^{t}Bu)
1,2 Addition	C_6F_6	14.1	2.6	22.4
	py_F	10.2	11.1	22.8
Cycloaddition	C_6F_6	>14.1	<7.5	26.2
	py_F	3.8	10.4	15.7

activation barrier is computed to be 11.1 kcal mol^{-1} for *o*-fluoropyridine, while for C_6F_6 this value drops dramatically to 2.6 kcal mol^{-1}. To further understand this discrepancy, we have analyzed the electrostatic potential (ESP) charge variations during the 1,2-CF addition step, using C_6F_6 as the substrate.[3] These ESP charge variations suggest that the reaction is enabled by donation of electron density from the nucleophilic alkylidyne carbon (or alkylidyne ligand) to the aromatic C_6F_6 since this substrate is easier to activate *via* an F-bound C_6F_6 adduct such as (PNP)Ti≡C^{t}Bu(σ-C_6F_6). In fact, C_6F_6 is in a sense a better electron accepter than *o*-fluoropyridine, hence the F-bound adduct is energetically preferred.

Taking into account the binding, activation, and solvation effects, the most difficult barrier for the *o*-fluoropyridine reaction profile, starting from intermediate **A**, is traversing through the **D-TS** (22.8 kcal mol^{-1}), a step which is similar to the largest barrier observed for C_6F_6 (22.0 kcal mol^{-1}). This means that overall, the 1,2-CF addition pathway is not unreasonable to propose at room temperature for either of the two substrates. However, the reason why each substrate most likely results in divergent pathways to C–F activation could be best interpreted by looking at the [2 + 2]-cycloaddition pathway. Hence we investigated this step for *o*-fluoropyridine, paying careful attention to intermediate **C**.

As noted above, complex **B** is an intermediate along the cycloaddition/β-F elimination pathway and the F moiety does not need to interact with the titanium center until after the cycloaddition step (Fig. 2), hence the C–F bond is not significantly activated simply by binding of pyridine *via* its nitrogen lone pair. However, in the [2 + 2]-cycloaddition pathway, the sp^2 C–F bond has been partially rehybridized and weakened. Fig. 5 illustrates the proposed structures for the [2 + 2]-cycloaddition product **C** and its transition state geometry leading to product **2**, (**C-TS**). When judge by its structure, **C-TS** is also early transition state, with Ti–F and C1–F distances of 2.82 Å and 1.78 Å, respectively. Intuitively, the C1–carbon in **C** has been partially rehybridized to sp^3, while the bond order calculations suggest the C1–F bond in these intermediates to be much weaker relative to the value computed for the free substrate. For example, the computed C1–F bond order in **C** is only 0.74, while the value observed for free *o*-fluoropyridine is much higher at 0.96. *Therefore, it appears that the sequential [2 + 2]-cycloaddition/β-F elimination pathway involves a C–F bond pre-activation step, specifically in the cycloaddition step. This event is not possible in the case of the 1,2-CF addition pathway, since the pyridine must dissociate first in order to isomerize to the F-bound titanium complex.*

As mentioned in our previous work,[3] we were unable to locate a minimum for the structure of C–F bound adduct of **A** with C_6F_6 ((PNP)Ti≡C^{t}Bu(σ-C_6F_6)), which ultimately leads to the [2 + 2]-cycloaddition species. We propose that the poor binding of C_6F_6 represents one of the critical factors that could disfavor the [2 + 2]-cycloaddition/β-F elimination pathway over the 1,2-CF bond addition pathway. In the case of *o*-fluoropyridine, the [2 + 2]-cycloaddition is benefited by the lone pair on the nitrogen atom, placing the *ortho*-carbon proximal and in line to the nucleophilic alkylidyne carbon. The computed binding free energy is as low as +3.8 kcal mol^{-1} (Table 1), and which translates to the most optimal binding amongst all the computed structures (adducts) that are relevant to C–F activation. This advantage ultimately results in a lower barrier for the [2 + 2]-cycloaddition/β-F elimination pathway rather than the 1,2-CF bond addition pathway. Based on our computation studies, we conclude that the *binding of the N-heterocycle is crucial for which pathway is preferred*.

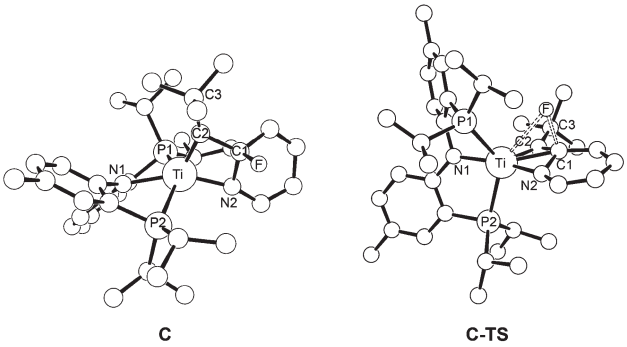

Fig. 5 Intermediate and transition state involving the β-fluoride elimination step (distance reported in Å). For **C**: Ti–F 3.31, Ti–C1 2.33, Ti–C2 1.84, Ti–P1 2.62, Ti–P2 2.66, Ti–N2 1.93, C1–F 1.48, C1–N2 1.48. For **C-TS**: Ti–F 2.82, Ti–C1 2.26, Ti–C2 1.85, Ti–P1 2.74, Ti–P2 2.61, Ti–N2 1.98, C1–F 1.78, C1–N2 1.42.

3. C–H *versus* C–F activation

The bond dissociation enthalpy for an aromatic C–H bond (~110 kcal mol^{-1})[12] is known to be much weaker than an aromatic C–F bond (~125 kcal mol^{-1}).[1] Despite this thermodynamic difference, activation of the C–F bond in *o*-fluoropyridine is preferred over the weaker C–H bond. To understand the selectivity in activating the strongest bond, we probed several reaction pathways one may expect in the event that C–H activation of the *N*-heterocycle would occur. As shown in Fig. 6, the energetically more favorable adduct $\mathbf{E_a}$ is responsible for the selectivity of the pathway involving sequential [2 + 2]-cycloaddition/β-H elimination pathway, which involves intermediate **F** and the C–H activated alkylidene final product $\mathbf{G_a}$. Following binding of *o*-fluoropyridine *via* its nitrogen lone pair, [2 + 2]-cycloaddition requires 11.3 kcal mol^{-1} to yield the proposed intermediate **F**, which is only 5 kcal mol^{-1} lower in energy relative to transient **A**. The rotational isomer $\mathbf{E_b}$, having the fluoride pointing towards the alkylidene ligand, plays no role in a hypothetical C–H bond activation pathway. Fig. 6 also illustrates how intermediate **F** can undergo β-hydride elimination to afford a hydride product $\mathbf{G_a}$. For this transformation to take place, however, a large energy penalty of 28.0 kcal mol^{-1} is required, and such barrier is much larger than the 5.6 kcal mol^{-1} required for the alternative β-F elimination pathway from **C** to form **2** (Fig. 2). The significantly larger β-H elimination barrier to afford $\mathbf{G_a}$ ultimately renders the cycloaddition/

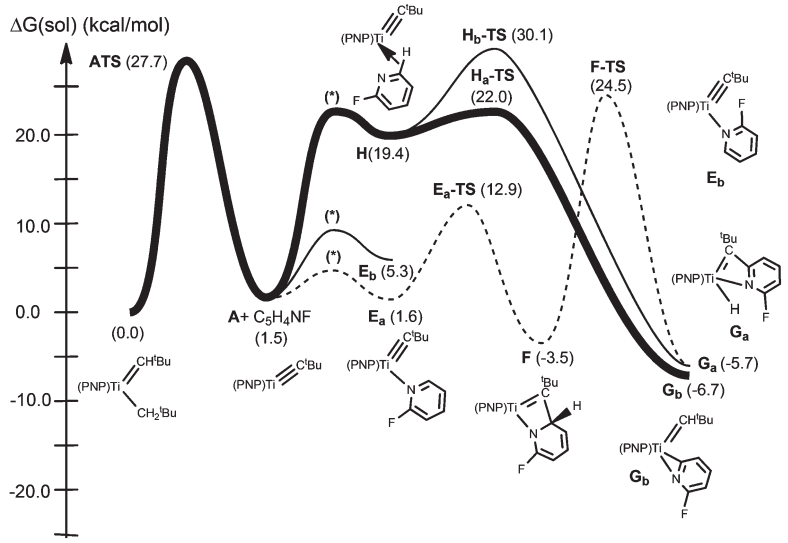

Fig. 6 C–H activation pathways for *o*-fluoropyridine.

β-H elimination C–H activation pathway less accessible than a [2 + 2]-cycloaddition/β-F elimination sequential pathway. The large barrier for β-H elimination is understandable because the acidic **H** of *o*-fluoropyridine must be migrated as a hydride. In the case of β-F elimination, the fluorine atom is migrated as fluoride, which renders the atom more easily transferrable. The driving force for C–F activation, 66.7 kcal mol^{-1} (Fig. 2), is also notable and far larger than that predicted for the C–H activation pathway to form $\mathbf{G_a}$ (5.7 kcal mol^{-1}). This discrepancy in driving force is mainly attributed to the inherent Ti–F bond strength as opposed to a reactive Ti–H bond.[13] In addition, for the system to enable the 1,2-addition of a C–H bond of *o*-fluoropyridine, such substrate should bind to titanium *via* its C–H bond. For this reorganization to occur, the substrate must coordinate to the metal center as shown in intermediate **H** (Fig. 6). As implied also by Fig. 6, the binding free energy of +17.9 kcal mol^{-1} suggests this interaction to be rather weak. Stemming from intermediate **H**, there are two likely 1,2-addition scenarios for how C–H activation can transpire. One pathway involves the 1,2-addition of the C–H bond *via* the negatively charged carbon to Ti, and positively charged H to the alkylidyne carbon (the fluoropyridyl product $\mathbf{G_b}$). This process *via* $\mathbf{H_a}$**-TS** is plausible based on Coulombic interactions, while the computed barrier for the addition step is only 2.6 kcal mol^{-1} to yield a relatively stable product being 6.7 kcal mol^{-1} lower in energy than the starting material (compound $\mathbf{G_b}$). The other addition pathway (*via* $\mathbf{H_b}$**-TS**) involves transfer of H to titanium and pyridyl transfer to the alkylidyne α-C, to form the product $\mathbf{G_a}$. As noted previously, this process is difficult since it requires a positively polarized hydrogen to be transferred as a hydride. As a result, the difference in energy between $\mathbf{H_a}$**-TS** and $\mathbf{H_b}$**-TS** is 8.1 kcal mol^{-1}, even though the products $\mathbf{G_a}$ and $\mathbf{G_b}$ are virtually isoenergetic. Therefore, the most reasonable 1,2-addition pathway for a hypothetical C–H bond activation of *o*-fluoropyridine is indicated in bold solid line in Fig. 6. Although the addition step only costs 2.6 kcal mol^{-1}, the binding of substrate to form **H** (+19.4 kcal mol^{-1}) is too poor such that its energy exceeds that for C–F activation (**B-TS**, +15.7 kcal mol^{-1}, *vide supra* Fig. 2). Binding of the substrate and not the bond activation, although a seemingly trivial step, appears to be the controlling factor behind the preference of C–F activation over the weaker C–H bond.

4. The role of the binding event in the ring-opening metathesis of *N*-heterocycles

From the data presented in this work we have established that the binding of an *N*-heterocycle (N bound, C–H bound, or C–F bound) dictates which reaction pathway will take place for the C–F bond activation. Combining our experimental results with our calculations we can assume that C–H activation of *N*-heterocycles such as pyridine is an unlikely event, while C–F bond activation in *o*-fluoropyridine will be the preferred site of activation. However, we have yet to consider ring-opening metathesis of *N*-heterocycles such as *o*-fluoropyridine since pyridine is known to undergo ring-opening in the presence of **A** to form the metallaazabicycle product shown in Scheme 3 (to give complex **3**).[9] This pathway might be much more favorable than our computed β-hydride elimination or 1,2-CH bond addition pathways depicted in Fig. 2 (dashed and solid bold lines, respectively). We know that 1,2-CH bond addition of pyridine to **A** to form an alkylidene pyridyl has a much higher barrier than the ring-opening metathesis pathway (Scheme 4). It has been computed that [2 + 2]-cycloaddition in **A-py** requires only a small barrier of 14 kcal mol^{-1} with a thermodynamic driving force of 1.7 kcal mol^{-1} (Scheme 4).[9a] This low barrier clearly outcompetes other possibilities shown in Fig. 6. Binding of pyridine to **A** (*via* the nitrogen lone pair) must be taking place

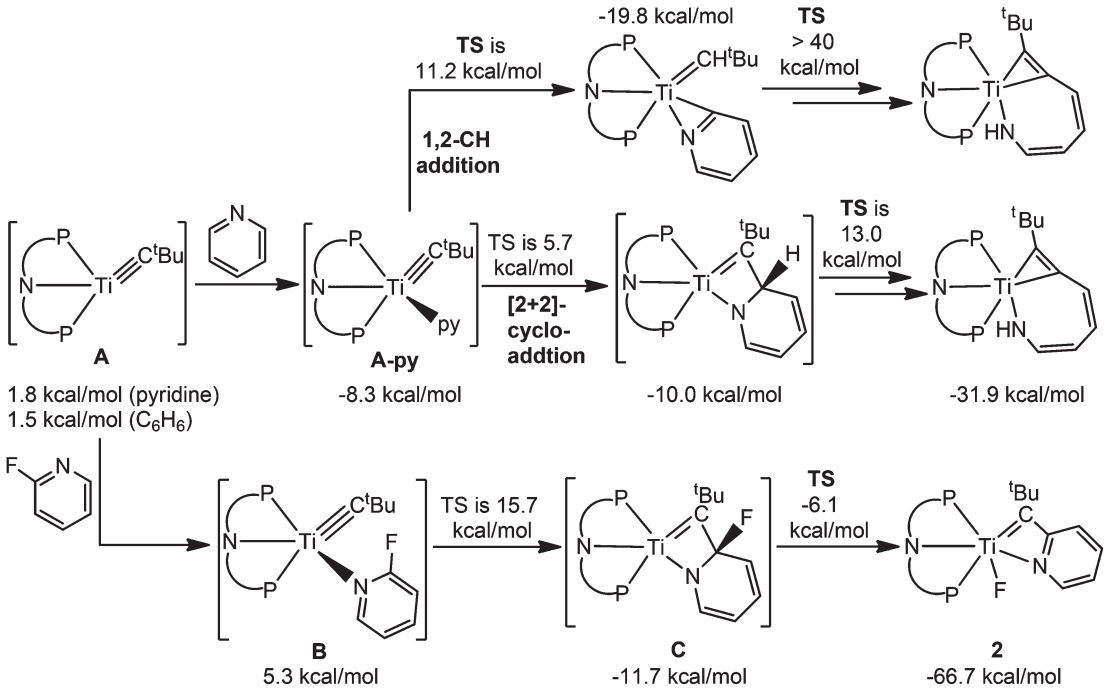

Scheme 4 1,2-CH addition, ring-opening metathesis, and 1,2-CF addition pathways involving **A** and the corresponding pyridine substrate. Activation energies are shown above reaction arrows while ΔG (solvation, kcal mol^{-1}) energies for intermediates and products are shown below each compound. Solution phase energies for compound **A** were computed using the dielectric constants (ε = 12.3 for pyridine, ε = 2.284 for C_6H_6) were used to simulate the solvent.

given that placement of fluoro groups in the *meta* position of pyridine does not appear to impede the ring-opening metathesis (Scheme 1, *vide supra*). When an *ortho* hydrogen is replaced with a fluoride group on the pyridine substrate the outcome of the reaction changes, even to the point of discouraging the ring-opening metathesis step. We propose that the barrier for ring-opening metathesis (13 kcal mol^{-1} computed for pyridine ring-opening, Fig. 2) is higher than the 5.6 kcal mol^{-1} energy needed for **C** to traverse to **2** (Fig. 2). Although we have not computed the energy needed for a hypothetical ring-opening metathesis of *o*-fluoropyridine, we anticipate that the energies of intermediates as well as activation barriers will not differ greatly since the difference in energies between **C** and the [2 + 2]-cycloaddition product between **A** and pyridine is only 1.7 kcal mol^{-1}.

5. Conclusions

In this work we have demonstrated that the binding mode of the substrate to transient **A** can alter the pathway significantly. For instance, arenes interact with the titanium center in **A** more so than alkanes, thus C–H bond activation takes place preferentially for the former C–H bonds (presumably *via* a π- and/or σ-C_6H_6 complex) despite these being more difficult to activate based purely on bond dissociation enthalpies. However, if binding of the substrate is too favored, as it is in the case of pyridine, C–H bond activation is penalized since the substrate must dissociate in order to place the C–H bond well in position with the nucleophilic alkylidyne carbon. As a result, the latter pathway is diverted *via* a [2 + 2]-cycloaddition and subsequent ring-opening metathesis among other low barrier steps. Unfortunately our proposed mechanism is not infallible, since we cannot discard inductive effects from playing a significant role in the case of fluoroarenes. When one combines the two features, pyridine and a fluoride, the outcome of the reaction depends on the position of the fluoride. When the fluoride is in the *ortho* position, [2 + 2]-cycloaddition is again favored, but the facile β-fluoride elimination pathway halts any chance for the system to undergo ring-open metathesis. Likewise, binding of the fluoropyridine substrate disfavors any chance of undergoing C–H bond activation *via* rearrangement to 1,2-CH bound linkage isomer.

6. Experimental section

General procedures

Unless otherwise stated, all operations were performed in a M. Braun Lab Master double-dry box under an atmosphere of purified nitrogen or using high vacuum standard Schlenk techniques under an argon atmosphere. Anhydrous *n*-hexane, pentane, toluene, and benzene were purchased from Aldrich in sure-sealed reservoirs (18 L) and dried by passage through two columns of activated alumina and a Q-5 column. Diethylether was dried by passage through a column of activated alumina. THF was distilled, under nitrogen, from purple sodium benzophenone ketyl and stored under sodium metal. Distilled THF was transferred under vacuum into thick walled reaction vessel before being transferred into a dry box.

C_6D_6 was purchased from Cambridge Isotope Laboratory (CIL), degassed and vacuum transferred to 4 Å molecular sieves. Celite, alumina, and 4 Å molecular sieves were activated under vacuum overnight at 200 °C. Compound (PNP)Ti=CH^{t}Bu ($CH_2{}^t$Bu) was prepared according to the literature.[7] All solvents used as reagents were dried by passage through an activated alumina column and if necessary, vacuum transferred from a CaH_2 mixture (which was stirred for 2 days). All other chemicals were used as received. CHN combustion analyses were performed by Desert Analytics, Tucson, AZ (USA). ^{1}H, ^{13}C, ^{31}B, ^{19}F, and ^{31}P NMR spectra were recorded on Varian 400 or 300 MHz NMR spectrometers. ^{1}H and ^{13}C NMR are reported with reference to residual solvent resonances (δ = 7.16 and 128.0 ppm for C_6H_6 in C_6D_6). ^{19}F NMR chemical shifts are reported with respect to external $HOCOCF_3$ (δ = −78.5 ppm). ^{31}P NMR chemical shifts are reported with respect to external H_3PO_4 (aqueous solution, δ = 0.0 ppm).

Preparation of complex 1. In a vial was dissolved (PNP)-Ti=CH^{t}Bu($CH_2{}^t$Bu) [102 mg, 0.165 mmol] in 2,6-difluoropyridine (~2 mL, excess, passed through a short column of alumina) at room temperature. The solution was allowed to stand for 3 days at room temperature where it changed from a green solution to a purple-blue solution and then was dried under vacuum. The residue was extracted with pentane and filtered. The filtrate was reduced in volume under reduced pressure, and then cooled to −35 °C. Purple needles of **1** [61 mg, 0.092 mmol, 56% yield] were collected.

For **1**: ^{1}H NMR (23 °C, 399.8 MHz, C_6D_6): δ 7.61 (dd, 1H, C_6H_3), 7.36 (dd, 1H, C_6H_3), 6.98 (d, 1H, C_6H_3), 6.87 (d, 1H, C_6H_3), 6.82 (d, 2H, C_6H_3), 6.74 (td, 1H, C_6H_3), 5.95 (d, 1H, Ti=C^{t}BuNC$_5H_3$F), 5.43 (d, 1H, Ti=C^{t}BuNC$_5H_3$F), 2.18 (s, 3H, $C_6H_3CH_3$), 2.15 (s, 3H, $C_6H_3CH_3$), 2.10–2.26 (m, 3H, C*H*Me$_2$), 2.00 (septet, 1H, C*H*Me$_2$), 1.71 (s, 9H, Ti=CC*Me*$_3$NC$_5H_3$F), 1.26 (dd, 9H, CH*Me*$_2$), 1.10 (dd, 3H, CH*Me*$_2$), 0.84–0.99 (m, 9H, CH*Me*$_2$), 0.55 (dd, 3H, CH*Me*$_2$). ^{13}C NMR (23 °C, 100.6 MHz, C_6D_6): δ 312.3 (Ti=*C*CMe$_3$NC$_5H_3$F), 167.7 (d, Ti=CCMe$_3$N*C*$_5H_3$F), 162.4 (d, C_6H_3), 160.5 (d, C_6H_3), 159.8 (Ti=CCMe$_3$N*C*$_5H_3$F), 142.0 (Ti=CCMe$_3$N*C*$_5H_3$F), 132.6 (C_6H_3), 132.3 (C_6H_3), 132.1 (C_6H_3), 131.6 (C_6H_3), 126.2 (d, C_6H_3), 125.1 (d, C_6H_3), 120.2 (dd, Ti=CCMe$_3$N*C*$_5H_3$F), 119.6 (d, C_6H_3), 119.4 (d, C_6H_3), 117.7 (d, C_6H_3), 104.4 (Ti=CCMe$_3$N*C*$_5H_3$F), 98.4 (d, C_6H_3), 42.3 (Ti=C*C*Me$_3$NC$_5H_3$F), 32.1 (Ti=CC*Me*$_3$NC$_5H_3$F), 26.7 (d, CHMe$_2$), 25.5 (d, CHMe$_2$), 21.2 (d, CHMe$_2$), 20.9 ($C_6H_3CH_3$), 20.7 ($C_6H_3CH_3$), 20.0 (d, CHMe$_2$), 19.9 (CHMe$_2$), 19.8 (CHMe$_2$), 18.9 (d, CHMe$_2$), 18.8 (CHMe$_2$), 18.2 (CHMe$_2$), 17.4 (CHMe$_2$), 17.2 (d, CHMe$_2$), 16.7 (d, CHMe$_2$). ^{31}P NMR (23 °C, 121.5 MHz, C_6D_6): δ 33.6 (dd, J_{P-P} = 50 Hz, J_{P-F} = 7 Hz), 29.4 (dd, J_{P-P} = 50 Hz, J_{P-F} = 7 Hz). ^{19}F NMR (23 °C, 282.3 MHz, C_6D_6): δ 202.3 (t, Ti–F, J_{P-F} = 28 Hz), −71.1 (d). Anal. Calcd. for $C_{36}H_{52}N_2P_2F_2Ti$: C, 65.45; H, 7.93; N, 4.24. Found: C, 65.18; H, 7.99; N, 3.61.

Preparation of complex 2. In a vial was dissolved (PNP)-Ti=CH^{t}Bu($CH_2{}^t$Bu) [80 mg, 0.130 mmol] in 2-fluoropyridine (~2 mL, excess, passed through a short column of alumina) at room temperature. The solution was allowed to stand for 2 days at room temperature where it changed from a green solution to a blue solution and then was dried under vacuum. The residue was extracted with pentane and filtered. The filtrate was reduced in volume under reduced pressure, and then cooled to −35 °C. The crude solution shows only small amounts of impurities, however crystallization gave complex **2** in a low crystalline yield [36 mg, 0.056 mmol, 43% yield]. Multiple attempts to obtain satisfactory elemental analysis failed.

For **2**: ^{1}H NMR (23 °C, 399.8 MHz, C_6D_6): δ 7.64 (d, 1H, Ar-*H*), 7.59 (dd, 1H, Ar-*H*), 7.36 (dd, 1H, Ar-*H*), 6.94 (br d, 1H, Ar-*H*), 6.78–6.88 (m, 4H, Ar-*H*), 6.24 (d, 1H, Ar-*H*), 5.84 (dd, 1H, Ar-*H*), 2.17 (s, 3H, $C_6H_3CH_3$), 2.15 (s, 3H, $C_6H_3CH_3$), 2.00–2.22 (m, 3H, C*H*Me$_2$), 1.83 (septet, 1H, C*H*Me$_2$), 1.73 (s, 9H, Ti=CC-*Me*$_3$NC$_5H_4$), 1.26–1.32 (m, 6H, CH*Me*$_2$), 1.10 (dd, 3H, CH*Me*$_2$), 0.86–0.94 (m, 9H, CH*Me*$_2$), 0.77 (dd, 3H, CH*Me*$_2$), 0.43 (dd, 3H, CH*Me*$_2$). ^{13}C NMR (23 °C, 100.6 MHz, C_6D_6): δ 313.6 (Ti=*C*C-Me$_3$NC$_5H_4$), 170.3 (Ti=CCMe$_3$N*C*$_5H_4$), 162.1 (d, C_6H_3), 160.5 (d, C_6H_3), 144.1 (Ti=CCMe$_3$N*C*$_5H_4$), 138.3 (Ti=CCMe$_3$N*C*$_5H_4$), 132.6 (C_6H_3), 132.5 (C_6H_3), 132.4 (C_6H_3), 132.1 (C_6H_3), 125.6 (d, C_6H_3), 124.9 (d, C_6H_3), 121.2 (d, C_6H_3), 120.5 (d, C_6H_3), 118.3 (d, C_6H_3), 117.8 (d, C_6H_3), 114.4 (Ti=CCMe$_3$N*C*$_5H_4$), 109.1 (Ti=CCMe$_3$N*C*$_5H_4$), 42.3 (Ti=C*C*Me$_3$NC$_5H_4$), 31.9 (Ti=CC*Me*$_3$NC$_5H_4$), 27.1 (d, CHMe$_2$), 25.1 (d, CHMe$_2$), 21.7 (d, CHMe$_2$), 20.9 ($C_6H_3CH_3$), 20.7 ($C_6H_3CH_3$), 19.8 (d, CHMe$_2$), 19.6 (CHMe$_2$), 19.5 (d, CHMe$_2$), 19.0 (CHMe$_2$), 18.9 (CHMe$_2$), 18.2 (d, CHMe$_2$), 17.9 (CHMe$_2$), 16.6 (CHMe$_2$), 16.5 (CHMe$_2$). ^{31}P NMR (23 °C, 121.5 MHz, C_6D_6): δ 32.5 (dd, J_{P-P} = 66 Hz, J_{P-F} = 13 Hz), 28.9 (dd, J_{P-P} = 66 Hz, J_{P-F} = 13 Hz). ^{19}F NMR (23 °C, 282.3 MHz, C_6D_6): δ 178.6 (t, J_{P-F} = 13 Hz, Ti–*F*).

Preparation of complex 3. In a vial was dissolved (PNP)-Ti=CH^{t}Bu($CH_2{}^t$Bu) [80 mg, 0.130 mmol] in 3-fluoropyridine (~2 mL, excess, passed through a short column of alumina) at room temperature. The solution was allowed to stand for 2 days at room temperature where it changed from a green solution to a red-brown solution and then was dried under vacuum. The residue was extracted with pentane and filtered. The filtrate was reduced in volume under reduced pressure, and then cooled to −35 °C. A brown solid was obtained in low yield and with some presence of free HPNP and another Ti(4+) product.

For **3**: ^{1}H NMR (23 °C, 399.8 MHz, C_6D_6): δ 9.9 (d, 1H, J = 11 Hz, (PNP)Ti(C(^{t}Bu)CCHCHCFCH-N*H*)), 7.62 (d, 1H, J = 10 Hz, (PNP)Ti(C(^{t}Bu)CC*H*CHCFCH-NH)), 7.35 (br s, 1H, (PNP)Ti(C-(^{t}Bu)CCHCHCFC*H*-NH)), 6.80 (br s, 1H, (PNP)Ti(C(^{t}Bu)-CCHC*H*CFCH-NH)), 2.19 (s, 6H, $C_6H_3CH_3$), 2.10 (m, 2H, C*H*Me$_2$), 1.86 (m, 2H, C*H*Me$_2$), 1.49 (s, 9H, ^{t}Bu), 1.29 (m, 6H, CH*Me*$_2$), 0.88 (m, 12H, CH*Me*$_2$), 0.56 (m, 6H, CH*Me*$_2$). ^{31}P NMR (23 °C, 121.5 MHz, C_6D_6): δ 35.3 (d, J_{P-P} = 56 Hz), 24.5 (d, J_{P-P} = 56 Hz). ^{19}F NMR (23 °C, 282.3 MHz, C_6D_6): δ −137.5 and −113.5 ppm. ^{13}C NMR spectra for this complex are rather uninformative given the presence of free ligand and another titanium product.

Single crystal X-ray diffraction details

Data collection of complex 1. The data collection was carried out using graphite monochromated Mo Kα radiation with a frame time of 64 seconds and a detector distance of

5.0 cm. A randomly oriented region of a sphere in reciprocal space was surveyed. Two sections of 606 frames were collected with 0.30° steps in ω at different ϕ settings with the detector set at −43° in 2θ. The predominate lattice was located using the Bruker RLATT program, and final cell constants were calculated from the xyz centroids of 543 strong reflections from the actual data collection after integration (SAINT).[14] In spite of the long scan times the number of observed data was extremely low, and combined with the presence of several minor components leads to very poor values for R_{sym}.

Structure solution and refinement for complex 1. Intensity statistics and systematic absences suggested the centrosymmetric space group $P2_1/c$ and subsequent solution and refinement confirmed this choice. The structure was solved using SHELXS-97 and refined with SHELXL-97.[15] A direct-methods solution was calculated which provided most non-hydrogen atoms from the E-map. Full-matrix least squares/difference Fourier cycles were performed which located the remaining non-hydrogen atoms. A hexane solvent is also present in the asymmetric unit. All non-hydrogen atoms were refined with anisotropic displacement parameters with the exception of the solvent carbon atoms.

Computational studies

All calculations were carried out using Density Functional Theory as implemented in the Jaguar 6.0 suite[16] of *ab initio* quantum chemistry programs. Geometry optimizations were performed with the B3LYP[17–20] functional and the 6-31G** basis set with no symmetry restrictions. Titanium was represented using the Los Alamos LACVP basis.[21,22] The energies of the optimized structures were reevaluated by additional single-point calculations on each optimized geometry using Dunning's correlation-consistent triple-ζ basis set,[23] cc-pVTZ-(-f) that includes a double set of polarization functions. For all transition metals, we used a modified version of LACVP, designated as LACV3P, in which the exponents were decontracted to match the effective core potential with the triple-ζ quality basis. Vibrational frequency calculations based on analytical second derivatives at the B3LYP/6-31G** (LACVP) level of theory were carried out on smaller models, to derive the zero-point-energy (ZPE) and entropy corrections at room temperature utilizing unscaled frequencies. Note that by entropy here we refer specifically to the vibrational/rotational/translational entropy of the solute(s); the entropy of the solvent is implicitly included in the dielectric continuum model. The molecules used for vibrational frequency calculations are derived from the corresponding fully optimized structure by replacing the methyl groups on the aromatic rings by H, and tertbutyl as well as isopropyl groups with methyl groups.

Solvation energies were evaluated by a self-consistent reaction field (SCRF)[24–26] approach based on accurate numerical solutions of the Poisson–Boltzmann equation.[27] In the results reported, solvation calculations were carried out at the optimized gas-phase geometry employing the dielectric constant of ε = 23.2 for *o*-fluoropyridine. The value 23.2 is actually the dielectric constant for *o*-bromopyridine. We did not find the experimental dielectric constant for *o*-fluoropyridine, instead we use the value for *o*-bromopyridine since a few known fluoro complexes have similar dielectric constant as bromo complexes (for examples, fluorobenzene 5.5, chlorobenzene 5.7, bromobenzene 5.4; *o*-fluorotoluene 4.2, *o*-chlorotoluene 4.7, *o*-bromotoluene 4.6). The minor error of the dielectric constant will not introduce significant errors to the theoretical results, since the computed reaction profile only varies very slightly with the dielectric constant. As an evidence, the shifts of the reaction profiles for C–F activation by **A** (Fig. 2) are within 0.5 kcal mol^{-1} by changing the dielectric constant from 23.2 to 12.3 (the value for pyridine).

The energy components have been computed following the protocol of our previous work.[28] The free energy in solution phase G(sol) were calculated as follows:[28]

$$G(\text{sol}) = G(\text{gas}) + G^{\text{solv}} \quad (1)$$

$$G(\text{gas}) = H(\text{gas}) - TS(\text{gas}) \quad (2)$$

$$H(\text{gas}) = H(\text{SCF}) + \text{ZPE} \quad (3)$$

G(gas) = free energy in gas phase; G^{solv} = free energy of solvation as computed using the continuum solvation model; H(gas) = enthalpy in gas phase; T = temperature (298.15 K); S(gas) = entropy in gas phase; H(SCF) = self consistent field energy, *i.e.* "raw" electronic energy as computed from the SCF procedure; ZPE = zero point energy.

The models used in this study consist of ~100 atoms, which represent the non-truncated substrates that were also used in the experimental work. Although a smaller model may also able to reproduce the most important features of the studied reaction qualitatively, we chose to employ the large scale model to faithfully construct realistic model chemistry. These calculations challenge the current state of computational capabilities. Whereas the numerical efficiency of the Jaguar program allows us to accomplish this task in a bearable time frame, vibrational frequency calculations, which are about an order of magnitude more expensive than geometry optimizations, are currently impossible to carry out on the large-scale model. As done in many of our previous large-scale simulation work, we have carefully made truncations to the substrate, where the decorations of the ligands were replaced with hydrogen and other minor modifications were made (these frequency-model structures are given below). We use these models only to derive the differential entropies.

Acknowledgements

We thank Indiana University-Bloomington, the Dreyfus Foundation, the Sloan Foundation, and the NSF (CHE-0848248 and CHE-0645381 to D.J.M.; CHE-0645381 to M.H.B.) for financial support of this research. A.R.F. acknowledges financial support from the College of Arts and Sciences (Dissertation Year Fellowship, Bernice Eastwood Covalt Memorial Scholarship, and the James H. Coon Science Prize). D.J.M. thanks

Dr Skye Fortier for insightful discussions especially regarding the molecular structure of complex **1**.

Notes and references

1 (*a*) B. E. Smart, in *The Chemistry of Functional Groups, Supplement D*, ed. S. Patai and Z. Rappoport, John Wiley & Sons, New York, 1983, ch. 14; (*b*) J. L. Kiplinger, T. G. Richmond and C. E. Osterberg, *Chem. Rev.*, 1994, **94**, 373; (*c*) J. Burdeniuc and R. H. Crabtree, *Chem. Ber./Recl.*, 1997, **130**, 145; (*d*) W. D. Jones, *Dalton Trans.*, 2003, 3991; (*e*) T. G. Richmond, in *Topics in Organometallic Chemistry*, ed. S. Murai, Springer, New York, 1999, vol. 3, p. 243; (*f*) A. Nova, R. Mas-Ballesté and A. Lledós, *Organometallics*, 2012, **31**, 1245; (*g*) S. A. Johnson, J. A. Hatnean and M. E. Doster, in *Progress in Inorganic Chemistry*, ed. K. D. Karlin, John Wiley & Sons, Inc., Hoboken, 2012, pp. 255–352; (*h*) M. Klahn and U. Rosenthal, *Organometallics*, 2012, **31**, 1235; (*i*) H. Amii and K. Uneyama, *Chem. Rev.*, 2009, **109**, 2119; (*j*) R. P. Hughes, *Eur. J. Inorg. Chem.*, 2009, 4591; (*k*) T. Braun and F. Wehmeier, *Eur. J. Inorg. Chem.*, 2011, 613; (*l*) E. Clot, O. Eisenstein, N. Jasim, S. A. Macgregor, J. E. McGrady and R. N. Perutz, *Acc. Chem. Res.*, 2011, **44**, 333; (*m*) A. D. Sun and J. A. Love, *Dalton Trans.*, 2010, **39**, 10362.

2 B. C. Bailey, J. C. Huffman and D. J. Mindiola, *J. Am. Chem. Soc.*, 2007, **129**, 5302.

3 J. G. Andino, H. Fan, A. R. Fout, B. C. Bailey, M.-H. Baik and D. J. Mindiola, *J. Organomet. Chem.*, 2011, **696**, 4138.

4 H. M. Hoyt, F. E. Michael and R. G. Bergman, *J. Am. Chem. Soc.*, 2004, **126**, 1018.

5 (*a*) C. C. Cummins, S. M. Baxter and P. T. Wolczanski, *J. Am. Chem. Soc.*, 1988, **110**, 8731; (*b*) C. C. Cummins, C. P. Schaller, G. D. Van Duyne, P. T. Wolczanski, A. W. E. Chan and R. Hoffmann, *J. Am. Chem. Soc.*, 1991, **113**, 2985; (*c*) C. P. Schaller and P. T. Wolczanski, *Inorg. Chem.*, 1993, **32**, 131; (*d*) J. L. Bennett and P. T. Wolczanski, *J. Am. Chem. Soc.*, 1994, **116**, 2179; (*e*) C. P. Schaller, J. B. Bonanno and P. T. Wolczanski, *J. Am. Chem. Soc.*, 1994, **116**, 4133; (*f*) L. M. Slaughter, P. T. Wolczanski, T. R. Klinckman and T. R. Cundari, *J. Am. Chem. Soc.*, 2000, **122**, 7953; (*g*) C. P. Schaller, C. C. Cummins and P. T. Wolczanski, *J. Am. Chem. Soc.*, 1996, **118**, 591; (*h*) J. L. Bennett and P. T. Wolczanski, *J. Am. Chem. Soc.*, 1997, **119**, 10696; (*i*) T. R. Cundari, T. R. Klinckman and P. T. Wolczanski, *J. Am. Chem. Soc.*, 2002, **124**, 1481; (*j*) D. F. Schafer II and P. T. Wolczanski, *J. Am. Chem. Soc.*, 1998, **120**, 4881; (*k*) P. J. Walsh, F. J. Hollander and R. G. Bergman, *J. Am. Chem. Soc.*, 1988, **110**, 8729; (*l*) B. A. Arndtsen, R. G. Bergman, T. A. Mobley and T. H. Peterson, *Acc. Chem. Res.*, 1995, **28**, 154; (*m*) A. P. Duncan and R. G. Bergman, *Chem. Rec.*, 2002, **2**, 431; (*n*) P. J. Walsh, F. J. Hollander and R. G. Bergman, *Organometallics*, 1993, **12**, 3705; (*o*) J. L. Polse, R. A. Andersen and R. G. Bergman, *J. Am. Chem. Soc.*, 1998, **120**, 13405; (*p*) S. Y. Lee and R. G. Bergman, *J. Am. Chem. Soc.*, 1995, **117**, 5877; (*q*) P. Royo and J. Sanchez-Nieves, *J. Organomet. Chem.*, 2000, **597**, 61; (*r*) J. de With and A. D. Horton, *Angew. Chem., Int. Ed. Engl.*, 1993, **32**, 903; (*s*) H. M. Hoyt and R. G. Bergman, *Angew. Chem., Int. Ed.*, 2007, **46**, 5580; (*t*) B. F. Wicker, H. Fan, A. K. Hickey, M. G. Crestani, J. Scott, M. Pink and D. J. Mindiola, *J. Am. Chem. Soc.*, 2012, **134**, 20081; (*u*) B. F. Wicker, J. Scott, A. R. Fout, M. Pink and D. J. Mindiola, *Organometallics*, 2011, **30**, 2453; (*v*) J. Scott, F. Basuli, A. R. Fout, J. C. Huffman and D. J. Mindiola, *Angew. Chem., Int. Ed.*, 2008, **47**, 8502.

6 (*a*) J. Cheon, D. M. Rogers and G. S. Girolami, *J. Am. Chem. Soc.*, 1997, **119**, 6804; (*b*) M. P. Coles, V. C. Gibson, W. Clegg, M. R. J. Elsegood and P. A. Porrelli, *Chem. Commun.*, 1996, 1963; (*c*) H. van der Heijden and B. Hessen, *J. Chem. Soc., Chem. Commun.*, 1995, 145; (*d*) C. B. Pamplin and P. Legzdins, *Acc. Chem. Res.*, 2003, **36**, 223; (*e*) K. Wada, C. B. Pamplin, P. Legzdins, B. O. Patrick, I. Tsyba and R. Bau, *J. Am. Chem. Soc.*, 2003, **125**, 7035; (*f*) K. Wada, C. B. Pamplin and P. Legzdins, *J. Am. Chem. Soc.*, 2002, **124**, 9680; (*g*) C. S. Adams, P. Legzdins and E. Tran, *Organometallics*, 2002, **21**, 1474; (*h*) C. S. Adams, P. Legzdins and W. S. McNeil, *Organometallics*, 2001, **20**, 4939; (*i*) C. S. Adams, P. Legzdins and E. Tran, *J. Am. Chem. Soc.*, 2001, **123**, 612; (*j*) J. Y. K. Tsang, M. S. A. Buschhaus, P. Legzdins and B. O. Patrick, *Organometallics*, 2006, **25**, 4215; (*k*) S. Zhang, M. Tamm and K. Nomura, *Organometallics*, 2011, **30**, 2712; (*l*) J. G. Andino, U. J. Kilgore, A. Ozarowski, J. Krzystek, J. Telser, M. Pink, M.-H. Baik and D. J. Mindiola, *Chem. Sci.*, 2010, **1**, 351.

7 (*a*) B. C. Bailey, H. Fan, E. W. Baum, J. C. Huffman, M.-H. Baik and D. J. Mindiola, *J. Am. Chem. Soc.*, 2005, **127**, 16016; (*b*) B. C. Bailey, H. Fan, J. C. Huffman, M.-H. Baik and D. J. Mindiola, *J. Am. Chem. Soc.*, 2007, **129**, 8781; (*c*) V. N. Cavaliere, M. G. Crestani, B. Pinter, C.-H. Chen, M. Pink, M.-H. Baik and D. J. Mindiola, *J. Am. Chem. Soc.*, 2011, **133**, 10700; (*d*) J. A. Flores, V. N. Cavaliere, D. Buck, G. Chen, M. G. Crestani, B. Pinter, M.-H. Baik and D. J. Mindiola, *Chem. Sci.*, 2011, **2**, 1457; (*e*) A. R. Fout, J. Scott, D. L. Miller, B. C. Bailey, J. C. Huffman, M. Pink and D. J. Mindiola, *Organometallics*, 2009, **28**, 331.

8 V. N. Cavaliere and D. J. Mindiola, *Chem. Sci.*, 2012, **3**, 3356–3365.

9 (*a*) B. C. Bailey, H. Fan, J. C. Huffman, M.-H. Baik and D. J. Mindiola, *J. Am. Chem. Soc.*, 2006, **128**, 6798; (*b*) B. C. Bailey, H. Fan, J. C. Huffman, M.-H. Baik and D. J. Mindiola, *J. Am. Chem. Soc.*, 2007, **129**, 7475; (*c*) A. R. Fout, B. C. Bailey, J. Tomaszewski and D. J. Mindiola, *J. Am. Chem. Soc.*, 2007, **129**, 12640; (*d*) A. Fout, B. C. Bailey, D. Buck, H. Fan, J. C. Huffman, M.-H. Baik and D. J. Mindiola, *Organometallics*, 2010, **29**, 5409.

10 (*a*) J. T. Ciszewski, B. Xie, C. Cao and A. L. Odom, *Dalton Trans.*, 2003, 4226; (*b*) K. S. Lokare, R. J. Staples and

A. L. Odom, *Organometallics*, 2008, **27**, 5130; (*c*) A. Fürstner, H. Krause, L. Ackermann and C. W. Lehmann, *Chem. Commun.*, 2001, 2240; (*d*) C. W. Bielawski, D. Benitez and R. H. Grubbs, *Science*, 2002, **297**, 2041; (*e*) C. W. Bielawski, D. Benitez and R. H. Grubbs, *J. Am. Chem. Soc.*, 2003, **125**, 8424.

11 See ESI.†

12 (*a*) W. D. Jones and F. J. Feher, *J. Am. Chem. Soc.*, 1982, **104**, 4240; (*b*) W. D. Jones, *Acc. Chem. Res.*, 2003, **36**, 140.

13 A. J. Hoskin and D. W. Stephan, *Coord. Chem. Rev.*, 2002, **233–234**, 107.

14 *SAINT 6.1*, Bruker Analytical X-Ray Systems, Madison, WI.

15 *SHELXTL-Plus V5.10*, Bruker Analytical X-Ray Systems, Madison, WI.

16 *Jaguar*, 5.5 ed, Schrödinger, L.L.C., Portland, OR, 1991–2003.

17 A. D. Becke, *Phys. Rev. A*, 1988, **38**, 3098.

18 A. D. Becke, *J. Chem. Phys.*, 1993, **98**, 5648.

19 C. T. Lee, W. T. Yang and R. G. Parr, *Phys. Rev. B: Condens. Matter*, 1988, **37**, 785.

20 S. H. Vosko, L. Wilk and M. Nusair, *Can. J. Phys.*, 1980, **58**, 1200.

21 P. J. Hay and W. R. Wadt, *J. Chem. Phys.*, 1985, **82**, 270.

22 W. R. Wadt and P. J. Hay, *J. Chem. Phys.*, 1985, **82**, 284.

23 T. H. Dunning, *J. Chem. Phys.*, 1989, **90**, 1007.

24 B. Marten, K. Kim, C. Cortis, R. A. Friesner, R. B. Murphy, M. N. Ringnalda, D. Sitkoff and B. Honig, *J. Phys. Chem.*, 1996, **100**, 11775.

25 M. Friedrichs, R. H. Zhou, S. R. Edinger and R. A. Friesner, *J. Phys. Chem. B*, 1999, **103**, 1190.

26 S. R. Edinger, C. Cortis, P. S. Shenkin and R. A. Friesner, *J. Phys. Chem. B*, 1997, **101**, 1190.

27 A. A. Rashin and B. Honig, *J. Phys. Chem.*, 1985, **89**, 5588.

28 M.-H. Baik and R. A. Friesner, *J. Phys. Chem. A*, 2002, **106**, 7407.

